ACS Medicinal Chemistry Letters

Letter

Synthesis of highly potent N-10 amino-linked DNA-alkylating indolinobenzodiazepine antibody-drug conjugates (ADCs)

Katie E Archer, Emily E Reid, Manami Shizuka, James Woods, Luke Harris, Erin K. Maloney, Laura M Bartle, Olga Ab, Alan Wilhelm, Yulius Setiady, Jose F. Ponte, Rajeeva Singh, Thomas A Keating, Ravi V.J. Chari, and Michael L Miller

ACS Med. Chem. Lett., **Just Accepted Manuscript** • DOI: 10.1021/acsmedchemlett.9b00254 • Publication Date (Web): 22 Jul 2019

Just Accepted

is published by the American Chemical Society. 1155 Sixteenth Street N.W., Washington, DC 20036

Synthesis of highly potent N-10 amino-linked DNA-alkylating indolinobenzodiazepine antibody-drug conjugates (ADCs)

Katie E. Archer, Emily E. Reid, Manami Shizuka,† James Woods,‡ Luke Harris, Erin K. Maloney, Laura M. Bartle, Olga Ab, Alan Wilhelm, Yulius Setiady, Jose F. Ponte, Rajeeva Singh, Thomas A. Keating, Ravi V.J. Chari, Michael L. Miller*

ImmunoGen, Inc., 830 Winter Street, Waltham, Massachusetts 02451, United States

KEYWORDS: Antibody-drug conjugates, ADCs, indolinobenzodiazepines.

ABSTRACT: Indolinobenzodiazepine DNA alkylators (IGNs) are the cytotoxic payloads in antibody-drug conjugates (ADCs) currently undergoing Phase I clinical evaluation (IMGN779, IMGN632, and TAK164). These ADCs possess linkers which have been incorporated into a central substituted phenyl spacer. Here we present an alternative strategy for the IGNs, linking through a carbamate at the readily available N-10 amine present in the monoimine containing dimer. As a result, we have designed a series of N-10 linked IGN ADCs with a wide range of *in vitro* potency and tolerability which may allow us to better match an IGN with a particular target based on the potential dosing needs.

A majority of antibody-drug conjugates (ADCs)[1-4] in clinical evaluation use tubulin-interacting agents, the maytansinoids and auristatins, as the cytotoxic payload.[5-6] Recently, there has been a surge of interest in payloads with alternative mechanisms of action, such as topoisomerase 1 inhibitors, exemplified by the camptothecins, and DNA crosslinkers, based on analogs of the pyrrolobenzodiazepine (PBD) dimer, SJG-136 (Figure 1).[7-9] Emerging clinical data indicate that doses achieved with these PBD ADCs are quite low, and treatment is often limited to two cycles because of toxic side effects.[10-11]

Previously, we disclosed a new DNA alkylator class, indolinobenzodiazepine pseudodimers (termed IGNs).[12-13] One major difference between the IGNs and PBDs is the mechanism of action. While, both PBDs and IGNs bind to the minor groove of DNA, only the PBDs, which contain a bis-imine, can crosslink with inter-strand guanine residues at preferred GATC sequences.[14] Through the controlled reduction of one of the two imine moieties, the IGNs are only capable of DNA alkylation, providing ADCs with improved tolerability in mice, and the potential to achieve higher doses in the clinic. The IGN component of all three ADCs of this payload class currently in clinical evaluation (IMGN779, IMGN632 and TAK164) share two additional structural features that are distinct from the PBDs: a) the pyrrolidine group was replaced with an indolino moiety, which results in tighter binding to DNA and a ~10-fold increase in *in vitro* cytotoxicity, b) the introduction of a substituted phenyl spacer instead of the propyl group between the two monomer sub-units which further increases potency, and provides a site for linker attachment (Figure 1).

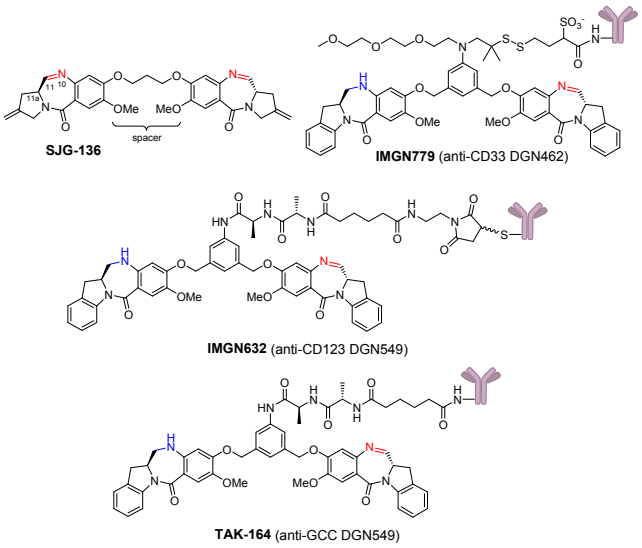

Figure 1. Structures of the DNA crosslinking PBD SJG-136 and the clinical stage ADCs of mono-reduced IGN DNA alkylators.

While this initial strategy allowed for rapid evaluation of a variety of linkers, we were limited in our ability to investigate the potential of extensive modification to the spacer group, and perhaps access to IGNs that would provide ADCs with a wider range of activity and tolerability. In order to explore the role of linkage position and spacer modification on preclinical activity as related to the IGN DNA alkylators, we synthesized a small set of IGNs, wherein, we fixed the linkage site at the N-10 amine of the reduced imine, while altering the spacer connecting the two monomer sub-units. Here, we report on the design, synthesis and preclinical evaluation of these N-10 linked IGN ADCs.

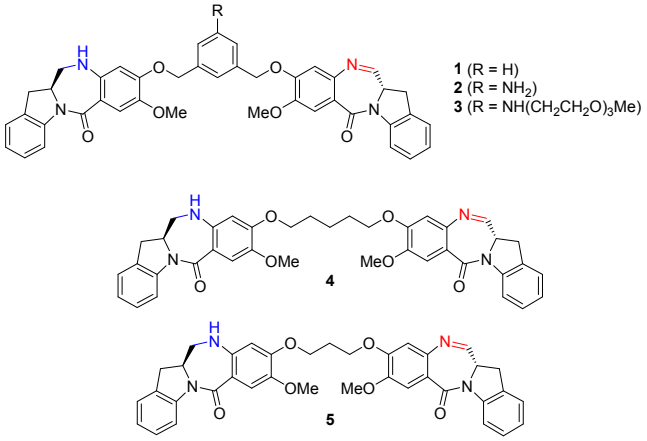

Figure 2. Structure of expected IGN catabolites.

Our modular synthetic strategy focused on structural modifications to the IGN psuedodimer to provide expected ADC catabolites with a wide range of *in vitro* potency. We designed and synthesized a small panel of these catabolites with spacers possessing either a phenyl group (**1**), a substituted phenyl (**2-3**), or an alkyl group (**4-5**) of different chain lengths (Figure 2). These catabolites were tested *in vitro* against the KB and Namalwa cell lines, and as expected, a range of potencies was observed. As shown in Table 1, the phenyl containing IGNs **1** and **2** demonstrated identical *in vitro* activity in the cell lines tested, whereas IGN **3**, with the larger and more polar PEG methyl ether substituent at the anilino nitrogen, was about 3-fold less potent in the KB cell line. IGN **5**, containing the three carbon propyl spacer, was found to be the least potent molecule in this series (10 to 30-fold less) *in vitro*. Interestingly, we found that increasing the spacer length from three carbons (**5**) to five (**4**) was accompanied by a significant increase in potency, which agrees well with previously reported data for the PBDs.[15] In fact, IGN catabolite **4**, with a five carbon pentyl spacer, was identical in potency to the phenyl substituted IGN **3**. In a separate study, we investigated the DNA binding capability of the catabolites in a competitive inhibition assay using a synthetic hairpin oligonucleotide (Figure 3). This study revealed that the catabolites possessing a substituted aromatic spacer (**2-3**) demonstrated superior DNA binding, perhaps accounting for the higher potency that was generally observed *in vitro*.

Table 1. In Vitro Potency of IGN catabolites 1-5[a]

Cell Line	Indication	Catabolite, IC_{50} pM				
		1	**2**	**3**	**4**	**5**
KB	cervical	8	8	20	20	200
Namalwa	lymphoma	1	2	3	3	30

[a]Cancer cell lines were incubated with ADCs for 5 days at 37°C. IC50 values were determined using a WST-based cell viability assay.

With a series of catabolites possessing a range of potencies in hand, we focused on developing a linking strategy. Using a design similar to that described in the literature for PBD ADCs, where the N-10 position is used as a linkage site,[8] we postulated that a self-immolative p-aminobenzyl (PAB) dipeptide could be used. In contrast to the PBDs which are linked via the imine at N-10, we chose to link IGNs **1-5** through a carbamate at the N-10 amino group; as upon ADC catabolism and linker cleavage, a monoimine IGN that is capable of alkylating DNA would be released. In addition, the presence of a free imine would allow for reversible sulfonation which enhances aqueous solubility, and facilitates conjugation to the antibody. In order to expand the usefulness of this synthetic approach we developed an unsymmetrical stepwise method, shown in Scheme 1, which differed from our previous synthetic methodology. (see Supplementary methods for the synthesis of catabolites **1-5**).

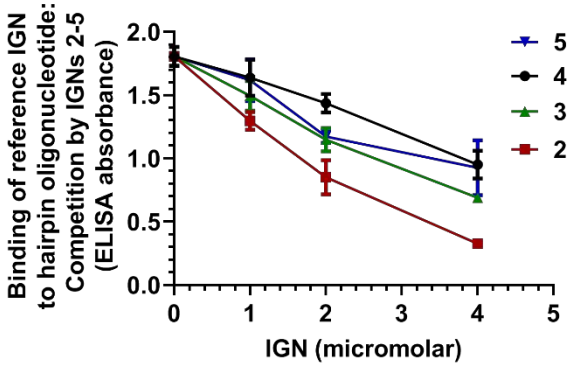

Figure 3. DNA interaction of IGN catabolites. Competitive inhibition by IGNs **2-5** at several concentrations to the binding of biotinylated reference IGN with digoxigenin-labeled hairpin oligonucleotide, measured as ELISA absorbance.

We prepared a set of IGNs wherein the dipeptide linker (e.g., Ala-Ala, Gln-Leu, Ala-Val) at the N-10 amino group was varied. As a general example, the synthesis of the Ala-Val methyl adipate IGN **12a** containing an N-hydroxysuccinimide (NHS) ester for conjugation to an antibody is described (Scheme 1). The methyl adipate Ala-Val dipeptide **6**, prepared through a four-step process, was converted to the corresponding p-aminobenzoyl derivative **7** in high yield by deprotection of the t-butyl ester with TFA followed by coupling with (4-aminophenyl)methanol using EEDQ. Treatment of the reduced IGN monomer **8** with 4-nitrobenzyl carbochloridate gave the activated carbamate **9** which was subsequently treated with alcohol **7** in the presence of LiHMDS to give the benzyl protected monomer **10** containing the desired linking group attached via the reduced N-10 amine. In a separate effort, a group of spacer modified imine containing IGN monomers (**a-c**) were prepared which contained either an alkyl iodide or bromide suitable for coupling reactions with a phenol.

Hydrogenolysis of benzyl protected monomer **10** using Pd/C generates the corresponding unprotected phenol which was then coupled with the iodopropyl IGN monomer (**a**) using potassium carbonate to give methyl ester **11a**. Hydrolysis of **11a** using lithium hydroxide to generate the carboxylic acid and treatment with N-hydroxysuccinimide gave the desired NHS ester **12a** in a 65% yield over two steps. With the successful preparation of NHS ester **12a**, conjugation was performed separately using either an anti-FRα or anti-EGFR antibody via lysine residues giving the ADCs anti-FRα **13a** and anti-EGFR **14a**, respectively. Through a similar set of transformations the anti-FRα (**13b-c**) and anti-EGFR (**14b-c**) ADCs possessing a self-immolative dipeptide linker at the N-10 amine and a variety of spacer groups were prepared. All conjugates had an average of

2.8 – 3.8 IGNs per antibody, were >97% monomeric by SEC and contained less than 0.5% unconjugated IGN (free drug).

Scheme 1. Synthesis of N-10 linked mono-reduced IGN ADCs with varying spacers.

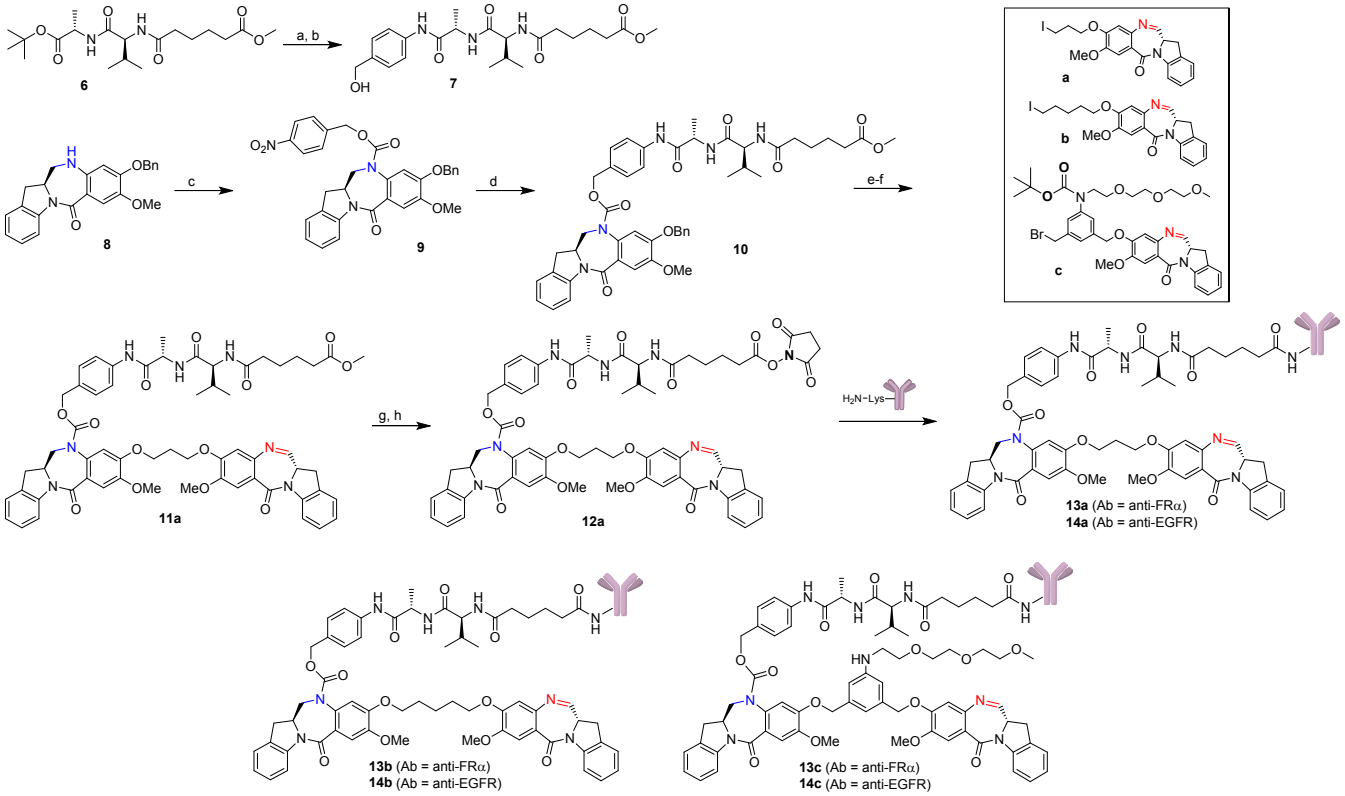

Reagents and Conditions: (a) TFA, water, 84%, (b) EEDQ, DCM, (4-aminophenyl)methanol, 31%, (c) DIPEA, DCM, 4-nitrobenzyl carbonochloridate, 71%, (d) **7**, LiHMDS, THF, 0 °C, ~35%, (e) Pd/C, H_2, CH_3OH, 77%, (f) **a**, K_2CO_3, DMA, 30%, (g) LiOH, THF/water, (h) N-hydroxysuccinimide, EDC, DCM, 65% over two steps.

Table 2. In Vitro Potency and tolerability of IGN ADCs

		ADC IC_{50} (pM)		
Anti-FRα		KB	T47D	Pilot MTD
ADC	DAR	(3,000k)[a]	(100k)[a]	mg/kg[b]
13a	2.9	100	>3000	>82
13b	2.8	10	100	~40
13c	3.3	20	300	~20

		ADC IC_{50} (pM)		
Anti-EGFR		HSC2	KB	NCI-H2110
ADC	DAR	(1,000k)[a]	(158k)[a]	(26k)[a]
14a	3.4	300	3000	>3000
14b	3.2	6	30	300
14c	3.8	6	40	100

[a]Number of antibody molecules bound per cell. [b]Dose based on mg/kg ADC.

The anti-FRα ADCs **13a-c** were evaluated against two cell lines which expressed either a high (KB) or low number (T47D) of folate antigen receptors. As shown in Table 2, potency of the ADCs was found to correlate with the *in vitro* cytotoxicity of the expected catabolites, and with the antigen level. Anti-FRα ADCs **13b-c** had comparable *in vitro* potency in both cell lines whereas ADC **13a,** incorporating catabolite **5**, was considerably less potent. Additionally, anti-FRα **13a** was found to be ineffective in the lower antigen expressing cell line T47D, indicating the need for high antigen expression to be active. Further evidence for this correlation was seen with the anti-EGFR ADCs **14a-c** when tested against three cells lines with varying antigen expression. Again, the correlation of ADC potency to the cytotoxicity of the catabolite and antigen expression level was similar to that observed for the anti-FRα ADCs **13a-c**. In all cases the ADCs were found to be antigen-specific as the addition of unconjugated Ab (1 μM) abolished all activity (see supplementary Table S1).

In addition to the impact of catabolite potency on ADC activity, we were also interested in determining its effect on bystander activity. We selected two cell lines, MDA-MB-468 (EGFR-positive) and Namalwa (EGFR-negative) to use in a bystander killing assay. *In vitro*, only the EGFR-positive MDA-MB-468 cells were sensitive to the anti-EGFR ADCs **14a-c,** demonstrating antigen specific cell killing by the ADC. A co-culture of MDA-MB-468 and Namalwa cells, representing the capacity of an ADC to kill tumors with heterogeneous antigen expression, was treated with ADCs **14a-c** (see supplementary Table S2). All three ADCs demonstrated potent bystander activity in this study, indicating that the direct killing of antigen

positive cells led to efficient generation of catabolites that were capable of diffusing into, and killing proximal antigen negative cells. Thus, the *in vitro* potency and bystander killing ability of these IGN ADCs were found to correlate with catabolite potency. We then conducted a pilot tolerability study in CD-1 mice. As shown in Table 2, the MTD (maximum tolerated dose) of the anti-FRα ADCs **13a-c** correlated with the observed *in vitro* activity, with the least potent ADC (**13a**) having the highest MTD.

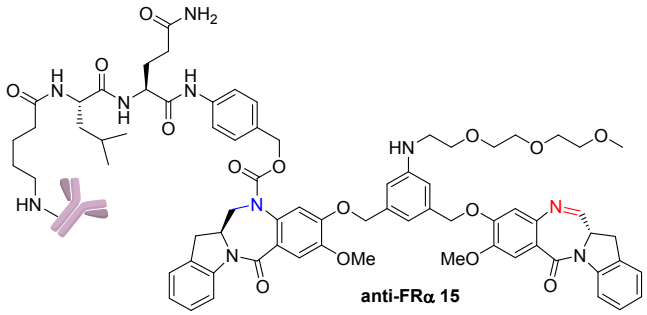

Figure 4. Structure of IGN ADC anti-FRα **15**.

Encouraged by the generation of a series of N-10 amine linked IGN ADCs which displayed a range of targeted *in vitro* potency, strong bystander activity and *in vivo* tolerability we next evaluated antitumor activity. For this study, we chose ADC **15**, which has a Gln-Leu linker, as this dipeptide was shown to be cleaved very efficiently by proteases in an *in vitro* screening assay. Anti-FRα ADC **15** (Figure 4), showed identical *in vitro* potency and tolerability to ADC **13c**, that has an Ala-Val dipeptide (see Supplementary Table S3). SCID mice bearing OV90 subcutaneous ovarian xenografts which express folate receptor alpha heterogeneously, at a very low level (H-Score 40)[16] were treated with ADC **15** (DAR 3.2). As shown in Figure 5, in spite of the low antigen expression level, the ADC was highly active, as treatment with a single i.v. dose of 0.7 mg/kg (equivalent to 15 μg/kg linked IGN **3** payload) resulted in 6/6 CRs with the higher doses (1.4 and 2.7 mg/kg) showing even greater activity. In this low expressing OV90 tumor model the anti-FRα **15** ADC demonstrated a therapeutic index (TI), defined as the ratio of MTD to MED (minimally effective dose), of >30.

Since our goal was to develop ADCs with a wide range of potency and tolerability, we then evaluated the anti-tumor activity of the less potent, but better tolerated, anti-EGFR ADC **14a** in a high antigen expressing model (Figure 6). Treatment of SCID mice bearing FaDu subcutaneous SCCHN xenografts (H-Score 225), with ADC **13a** at a single i.v. dose of 3.7 mg/kg (equivalent to 80 μg/kg of the IGN **5** payload) resulted in high activity, with 6/6 CRs, indicating that efficient antitumor activity is achievable with a lower potency IGN payload when the antigen expression level is properly matched.

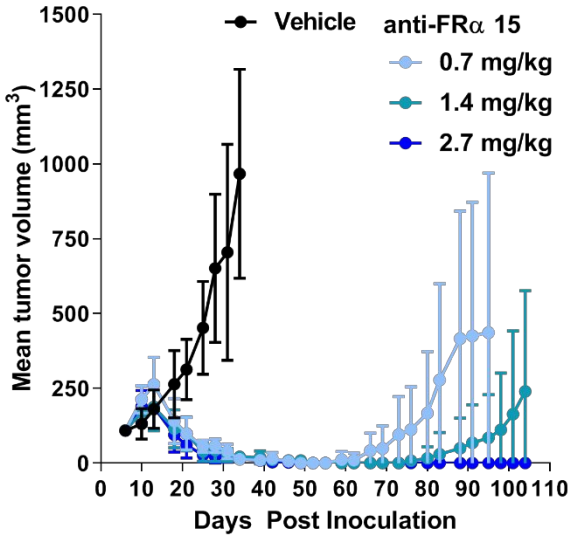

Figure 5. *In vivo* antitumor activity of the anti-FRα **15** ADC in an ovarian cancer OV90 xenograft.

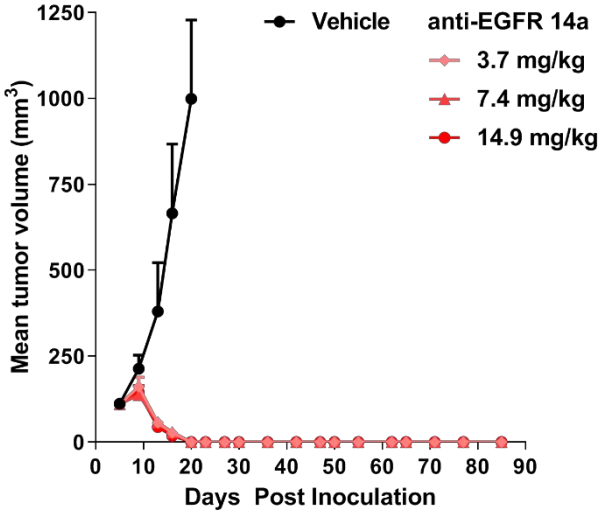

Figure 6. *In vivo* antitumor activity of the anti-EGFR **20** ADC in a squamous cell carcinoma of the head and neck FaDu Xenograft.

In conclusion, we have developed a new linking strategy for IGNs using the N-10 amine present in our monoimine containing IGN pseudodimers. This has allowed us to explore the impact of incorporating variable spacer units leading to the synthesis of IGN ADCs which demonstrate a wide range of *in vitro* potency that correlates with bystander activity and *in vivo* tolerability. As a result, we can use this information to better select an IGN for generating an ADC based on the needs of the target, as demonstrated by the potent antitumor activity for the anti-FRα **15** ADC, where antigen expression is low and potent bystander activity is needed, and the anti-EGFR **14a** ADC where the antigen expression in the xenograft model is high.

ASSOCIATED CONTENT

Supporting Information

The Supporting Information is available free of charge on the ACS Publications website at DOI:.

Detailed experimental procedures for all compounds and ADCs. (PDF)

AUTHOR INFORMATION

Corresponding Author

* E-mail: michael.miller@immunogen.com

Present Address

†Pharmaron, Inc., Waltham, MA 02451. ‡Alkermes, Inc., Waltham, MA 02451.

Author Contributions

The manuscript was written through contributions of all authors. All authors of submitting affiliation have given approval to the final version of the manuscript.

Funding Sources

This study was supported by ImmunoGen, Inc.

ABBREVIATIONS

ADC, antibody-drug conjugate; PBD, pyrrolobenzodiazepine; IGN, indolinobenzodiazepine; TMDD, target mediated drug disposition; PAB, p-aminobenzoyl; TFA, triflouoroacetic acid; EEDQ, N-ethoxycarbonyl-2-ethoxy-1,2-dihydroquinoline; DCM, dichloromethane; DIPEA, N,N-Diisopropylethylamine; THF, tetrahydrofuran; DMSO, dimethylsulfoxide; DMA, dimethylacetmide; NHS, N-hydroxysuccinimide ester; EDC, 1-Ethyl-3-(3-dimethylaminopropyl)carbodiimide; SEC, size-exclusion chromatography; DAR, drug-to-antibody ratio; MTD, maximum tolerated dose; MED, minimum effective dose; CR, complete regression.

REFERENCES

(1) Chari, R. V.; Miller, M. L.; Widdison, W. C. Antibody-drug conjugates: an emerging concept in cancer therapy. *Angew. Chem. Int. Ed. Engl.* **2014**, 53, 3796-827.

(2) Beck, A.; Goetsch, L.; Dumontet, C.; Corvaia, N. Strategies and challenges for the next generation of antibody-drug conjugates. *Nat. Rev. Drug Discov.* **2017**, 16, 315-337.

(3) Polakis, P. Antibody Drug Conjugates for Cancer Therapy. *Pharmacol. Rev.* **2016**, 68, 3-19.

(4) Coats, S; Williams, M.; Kebble, B.; Dixit, R.; Tseng, L.; Yao, N.; Tice, D.A.; Soria, J-C. Antibody Drug Conjugates: Future Directions in Clinical and Translational Strategies to Improve the Therapeutic Index. *Clin. Cancer Res.* **2019**, doi: 10.1158/1078-0432.CCR-19-0272.

(5) Chari, R. V. Expanding the Reach of Antibody-Drug Conjugates. *ACS Med. Chem. Lett.* **2016**, 7, 974-976.

(6) Sievers, E. L., Senter, P. D. Antibody-drug conjugates in cancer therapy. *Annu. Rev. Med.* **2013**, 64, 15-29.

(7) Ogitani, Y.; Aida, T.; Hagihara, K.; Yamaguchi, J.; Ishii, C.; Harada, N.; Soma, M.; Okamoto, H.; Oitate, M.; Arakawa, S.; Hirai, T.; Atsumi, R.; Nakada, T.; Hayakawa, I.; Abe, Y.; Agatsuma, T. DS-8201a, A Novel HER2-Targeting ADC with a Novel DNA Topoisomerase I Inhibitor, Demonstrates a Promising Antitumor Efficacy with Differentiation from T-DM1. *Clin. Cancer Res.* **2016**, 22, 5097-5108.

(8) Mantaj, J.; Jackson, P. J.; Rahman, K. M.; Thurston, D. E. From Anthramycin to Pyrrolobenzodiazepine (PBD)-Containing Antibody-Drug Conjugates (ADCs). *Angew. Chem. Int. Ed. Engl.* **2017**, 56, 462-488.

(9) Hartley, J. A.; Spanswick, V. J.; Brooks, N.; Clingen, P. H.; McHugh, P. J.; Hochhauser, D.; Pedley, R. B.; Kelland, L. R.; Alley, M. C.; Schultz, R.; Hollingshead, M. G.; Schweikart, K. M.; Tomaszewski, J. E.; Sausville, E. A.; Gregson, S. J.; Howard, P.W.; Thurston, D. E. SJG-136 (NSC 694501), a novel rationally designed DNA minor groove interstrand cross-linking agent with potent and broad spectrum antitumor activity: part 1: cellular pharmacology, in vitro and initial in vivo antitumor activity. *Cancer Res.* **2004**, 64, 6693.

(10) Stein, E. M.; Walter, R. B.; Erba, H. P.; Fathi, A. T.; Advani, A. S.; Lancet, J. E.; Ravandi, F.; Kovacsovics, T.; DeAngelo, D. J.; Bixby, D.; Faderl, S.; Jillella, A. P.; Ho, P. A.; O'Meara, M. M.; Zhao, B.; Biddle-Snead, C.; Stein, A. S. A phase 1 trial of vadastuximab talirine as monotherapy in patients with CD33-positive acute myeloid leukemia. *Blood* **2018**, 131, 387-396.

(11) Rudin, C. M.; Pietanza, M. C.; Bauer, T. M.; Ready, N.; Morgensztern, D.; Glisson, B. S.; Byers, L. A.; Johnson, M. L.; Burris, H. A., 3rd; Robert, F.; Han, T. H.; Bheddah, S.; Theiss, N.; Watson, S.; Mathur, D.; Vennapusa, B.; Zayed, H.; Lally, S.; Strickland, D. K.; Govindan, R.; Dylla, S. J.; Peng, S. L.; Spigel, D. R.; investigators, S. Rovalpituzumab tesirine, a DLL3-targeted antibody-drug conjugate, in recurrent small-cell lung cancer: a first-in-human, first-in-class, open-label, phase 1 study. *Lancet Oncol.* **2017**, 18, 42-51.

(12) Miller, M. L.; Fishkin, N. E.; Li, W.; Whiteman, K. R.; Kovtun, Y.; Reid, E. E.; Archer, K. E.; Maloney, E. K.; Audette, C. A.; Mayo, M. F.; Wilhelm, A.; Modafferi, H. A.; Singh, R.; Pinkas, J.; Goldmacher, V.; Lambert, J. M.; Chari, R. V. A New Class of Antibody-Drug Conjugates with Potent DNA Alkylating Activity. *Mol. Cancer Ther.* **2016**, 15, 1870-8.

(13) Miller, M. L.; Shizuka, M.; Wilhelm, A.; Salomon, P.; Reid, E. E.; Lanieri, L.; Sikka, S.; Maloney, E. K.; Harvey, L.; Qiu, Q.; Archer, K. E.; Bai, C.; Vitharana, D.; Harris, L.; Singh, R.; Ponte, J. F.; Yoder, N. C.; Kovtun, Y.; Lai, K. C.; Ab, O.; Pinkas, J.; Keating, T. A.; Chari, R. V. J. A DNA-Interacting Payload Designed to Eliminate Cross-Linking Improves the Therapeutic Index of Antibody-Drug Conjugates (ADCs). *Mol. Cancer Ther.* **2018**, 17, 650-660.

(14) Rahman, K. M.; James, C. H.; Thurston, D. E. Effect of base sequence on the DNA cross-linking properties of pyrrolobenzodiazepine (PBD) dimers. *Nucleic Acids Res*. **2011**, 39, 5800–5812.

(15) Gregson, S. J.; Howard, P.W.; Gullick, D. R.; Hamaguchi, A.; Corcoran, K. E.; Brooks, N. A.; Hartley, J. A.; Jenkins, T. C.; Patel, S.; Guille, M. J.; Thurston, D. E. Linker Length Modulates DNA Cross-Linking Reactivity and Cytotoxic Potency of C8/C8‘ Ether-Linked C2-exo-Unsaturated Pyrrolo[2,1-c][1,4]benzodiazepine (PBD) Dimers. *J. Med. Chem.* **2004** , 47, 1161-1174.

(16) Detre, S.; Saclani, J. G.; Dowsett, M. A. A "quickscore" method for immunohistochemical semiquantitation: validation for oestrogen receptor in breast carcinomas. *J Clin Pathol.* **1995**, 48 , 876-8.

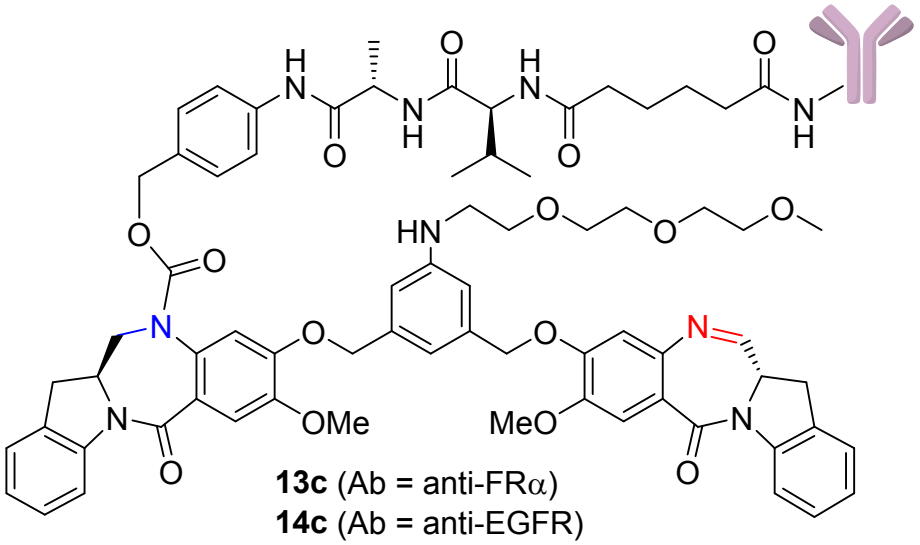

13c (Ab = anti-FRα)
14c (Ab = anti-EGFR)